

Semi-implicit methods for advection equations with explicit forms of numerical solution.

Peter Frolkovič · Svetlana Krišková ·
Michaela Rohová · Michal Žeravý

Received: June 30, 2021/ Accepted: The correct dates will be entered by the editor

Abstract We present a parametric family of semi-implicit second order accurate numerical methods for non-conservative and conservative advection equation for which the numerical solutions can be obtained in a fixed number of forward and backward alternating substitutions. The methods use a novel combination of implicit and explicit time discretizations for one-dimensional case and the Strang splitting method in several dimensional case. The methods are described for advection equations with a continuous variable velocity that can change its sign inside of computational domain. The methods are unconditionally stable in the non-conservative case for variable velocity and for variable numerical parameter. Several numerical experiments confirm the advantages of presented methods including an involvement of differential programming to find optimized values of the variable numerical parameter.

Keywords advection equation · semi-implicit method · unconditional stability · conservation laws

1 Introduction

Implicit (or semi-implicit) numerical schemes are useful numerical methods to solve advection dominated problems in several circumstances [1, 2, 3, 4, 5, 6, 7, 8, 10, 14, 15, 17, 18, 19, 20, 22]. They can avoid or reduce significantly the main disadvantage of fully explicit schemes that are implemented on a fixed mesh with a finite stencil in numerical discretization. Such explicit schemes based on finite difference or finite volume methods require a stability restriction on the choice

The work was supported by the grant VEGA 1/0709/19 and APVV-19-0460.

Peter Frolkovič · Svetlana Krišková · Michaela Rohová · Michal Žeravý
Dept. of Mathematics and Descriptive Geometry, Faculty of Engineering STU
Radlinského 11, 810 05 Bratislava, Slovakia
E-mail: peter.frolkovic@stuba.com

of discretization parameters [11], e.g. the time step. This can be disadvantageous in several situations like highly variable velocity field or nonuniform space discretization step [4,13] or long time simulations when approaching stationary solutions [19]. Another important type of problems when implicit schemes can be useful are stiff differential equations involving the advection term [3,9,10,15].

In an ideal case, the implicit and semi-implicit methods can offer an unconditional stability that make them convenient tool to solve numerically the problems having previously mentioned complications. The price to pay is that the numerical solution must be obtained in general by solving linear algebraic system of equations. Our aim is to propose a semi-implicit second order accurate numerical method having unconditional stability where the obtained linear systems can be solved in a small given number of alternating substitutions. Consequently, such scheme can compete well with fully explicit schemes that themselves lack the advantage of unconditional stability.

In [4] a novel parametric family of semi-implicit second order accurate numerical schemes for linear non-conservative advection is introduced. We base our work here on this result that is extended in several aspects. We treat here only representative advection equations, but the derived numerical schemes can be used for more involved advection dominated problems.

Additionally to [4], we show how one-dimensional discretized problems with a velocity that can change its sign several times in domain can be solved by one forward and one backward substitution as known for so called fast sweeping methods [12,23]. The derivation of second order scheme is based here on the discretization of an error term for the fully implicit first order accurate upwind scheme. Consequently, it is easy to apply some limiter procedures based on a blending between these two types of schemes if necessary. The free parameter of this family of schemes is introduced in a more convenient way than in [4]. The parameter can vary in space and time that we demonstrate in one numerical experiment by letting find its optimized values using differential programming tools.

In this work we present for the first time the semi-implicit scheme also for the linear advection equation in the conservative form. The scheme is based on finite volume method and it offers an exact local mass balance property in a discrete form that is confirmed also by numerical experiments. Nevertheless, to insure such property, the local variability of the parameter in the method is not allowed and the unconditional von Neumann stability can be shown only for constant velocity case. Therefore, if the advection dominated problem can be expressed in a non-conservative form, e.g. for the divergence free velocity, we prefer the more flexible semi-implicit non-conservative method. As confirmed by several numerical experiments, the errors in mass balance for chosen numerical examples diminish fast with a mesh refinement.

Finally, we apply the derived one-dimensional non-conservative scheme for two-dimensional advection equation using Strang splitting [11,21] that preserves the second order accuracy. Such treatment requires to solve only a given number of one-dimensional problems in alternating directions that can

be solved by our proposed numerical scheme. One can show that such splitting scheme preserves the property of unconditional stability [21] that is not the case of unsplit version presented in [4].

We proceed as follows. In Section 2 we derive the parametric family of one-dimensional semi-implicit non-conservative advection scheme. In Section 3 we derive analogous conservative advection schemes. In Section 4 we introduce the Strang splitting for problems in two dimension that preserves the accuracy and the unconditional stability of 1D scheme. In Section 5 we illustrate all properties on several numerical examples.

2 Non-conservative advection equation

The linear advection equation in the non-conservative form is given by

$$\partial_t \phi + v \partial_x \phi = 0, \quad \phi(x, 0) = \phi^0(x), \quad (1)$$

where the velocity function $v = v(x)$ is a given continuous function. The unknown function $\phi = \phi(x, t)$ is prescribed at $t = 0$ by the given function $\phi^0 = \phi^0(x)$ and $\phi(x, t)$ should be determined for $t > 0$ and $x \in (0, L) \subset R$. The boundary values are prescribed by given functions $\phi_0 = \phi_0(t)$ and $\phi_L = \phi_L(t)$ only if an inflow situation occurs at the boundary, namely,

$$\phi(0, t) = \phi_0(t), \text{ if } v(0) \geq 0, \quad \phi(L, t) = \phi_L(t), \text{ if } v(L) \leq 0. \quad (2)$$

The model equation (1) can be solved by finding so called characteristic curves, the characteristics, generated by v and using the fact that the solution ϕ is constant along characteristics [11].

In what follows, we use the following common notations of finite difference methods. We denote $x_i = ih$, $i = 0, 1, \dots, I$ for a chosen I , where $h = L/I$, and $t^n = n\tau$, $n = 0, 1, \dots, N$ for a chosen N and $\tau > 0$. Our aim is to find the approximations ϕ_i^n of $\phi(x_i, t^n)$. The initial values are given by $\phi_i^0 = \phi^0(x_i)$, and for $i = 0$ and $i = I$ they can be replaced by the values using the boundary conditions (2).

Remark 1 To simplify our presentation, we consider a particular form of the velocity v being a piecewise linear function of x that can be determined by its discrete values $v_i = v(x_i)$ for each mesh. Such situation is typical if the velocity field is obtained by a numerical solution of some flow equation or when the velocity function is approximated from its values in mesh points. We allow that the velocity can change its sign inside of $(0, L)$ when the points for which $v = 0$ can be then easily determined from its piecewise linear form.

Later we distinguish the case of so called expanding characteristics for points $\bar{x} \in (x_i, x_{i+1})$ such that $v(\bar{x}) = 0$ and $v'(\bar{x}) > 0$. In this case, the regions $x \leq \bar{x}$ and $x \geq \bar{x}$ are "separated" from each other that may require a special treatment in numerical schemes, see later. Note that if the velocity v in (1) depends also on t , we use an approximation by fixing its value on each time subinterval $[t^n, t^{n+1}]$ using a representative value, e.g., at $t = t^n + \tau/2$.

In such case, the positions of zero points \bar{x} have to be redetermined in each time subinterval.

2.1 First order accurate fully implicit scheme

The scheme can be derived using the backward Euler method for the time discretization and the upwind one-sided finite difference for the space discretization,

$$\frac{\phi_i^{n+1} - \phi_i^n}{\tau} + v_i^+ \frac{\phi_i^{n+1} - \phi_{i-1}^{n+1}}{h} + v_i^- \frac{\phi_{i+1}^{n+1} - \phi_i^{n+1}}{h} = 0,$$

where $v^+ := \max\{0, v\}$ and $v^- := \min\{0, v\}$. Denoting (signed) Courant numbers at mesh points

$$C_i := \frac{\tau v_i}{h}, \quad (3)$$

we can write the scheme in the concise form

$$\phi_i^{n+1} = (1 + |C_i|)^{-1} (\phi_i^n + |C_i| \phi_{i\mp 1}^{n+1}) \quad (4)$$

with $\mp = -\text{sgn}(C_i)$. The scheme (4) can be used for $n = 0, 1, \dots, N$ and for the inner nodes with $i = 1, 2, \dots, I-1$. For boundary nodes one applies either the Dirichlet boundary conditions (2),

$$\phi_0^{n+1} = \phi_0(t^{n+1}), \quad \text{if } C_0 \geq 0, \quad (5)$$

$$\phi_I^{n+1} = \phi_L(t^{n+1}), \quad \text{if } C_I \leq 0, \quad (6)$$

or one simplifies (4) for the outflow boundaries to

$$\phi_0^{n+1} = (1 - C_0)^{-1} (\phi_0^n - C_0 \phi_1^{n+1}), \quad \text{if } C_0 < 0, \quad (7)$$

$$\phi_I^{n+1} = (1 + C_I)^{-1} (\phi_I^n + C_I \phi_{I-1}^{n+1}), \quad \text{if } C_I > 0. \quad (8)$$

Finally, we modify (4) for the special case of expanding characteristics as described in Remark 1. Namely, if there exists i^* such that

$$v_{i^*} < 0 \quad \text{and} \quad v_{1+i^*} > 0,$$

then there is a point $\bar{x}_{i^*} \in (x_{i^*}, x_{1+i^*})$ where the piecewise linear velocity attains the zero value. For such point with expanding characteristics we decouple the computations of $\phi_{i^*}^{n+1}$ and $\phi_{1+i^*}^{n+1}$ from each other. Namely, the scheme (4) is replaced for $i = i^*$ and $i = 1 + i^*$ by the explicit definitions

$$\begin{aligned} \phi_{i^*}^{n+1} &= (1 - C_{i^*})^{-1} (\phi_{i^*}^n - C_{i^*} \phi_{i^{**}}^n), \\ \phi_{1+i^*}^{n+1} &= (1 + C_{1+i^*})^{-1} (\phi_{1+i^*}^n + C_{1+i^*} \phi_{i^{**}}^n). \end{aligned} \quad (9)$$

To use it, we determine the location of \bar{x}_{i^*} from the linear interpolation,

$$\bar{x}_{i^*} = x_{i^*} + \frac{v_{i^*}}{v_{i^*} - v_{1+i^*}} h.$$

Afterwards, we define the interpolated value $\phi_{i^{**}}^n \approx \phi(\bar{x}_{i^*}, t^n)$ by

$$\phi_{i^{**}}^n := \phi_{i^*}^n + \frac{\bar{x}_{i^*} - x_{i^*}}{h} (\phi_{1+i^*}^n - \phi_{i^*}^n)$$

and

$$C_{1+i^*} := \frac{\tau v_{1+i^*}}{x_{1+i^*} - \bar{x}_{i^*}}, \quad C_{i^*} := \frac{\tau v_{i^*}}{\bar{x}_{i^*} - x_i}.$$

The schemes (9) is then determined using the approximation that $\phi(x_{i^*}, t) \equiv \phi_{i^{**}}^n$ for $t \in [t^n, t^{n+1}]$ as $v(\bar{x}_{i^*}) = 0$.

Formally, the schemes (4) - (9) represent a system of linear algebraic equations. Nevertheless, each i -th equation in (4) - (9) contains at most one neighbor value, either ϕ_{i-1}^{n+1} or ϕ_{i+1}^{n+1} (or none). Such linear equations can be solved using one forward and backward substitution as known for fast sweeping methods [23].

Alternatively, one can formulate the substitutions analogously to [12] when the discrete equations are split into two fractional steps that must be applied in the defined order for i , namely

$$\phi_i^{n+1/2} = (1 + C_i^+)^{-1} (\phi_i^n + C_i^+ \phi_{i-1}^{n+1}), \quad i = 0, 1, \dots, I \quad (10)$$

$$\phi_i^{n+1} = (1 - C_i^-)^{-1} (\phi_i^{n+1/2} - C_i^- \phi_{i+1}^{n+1}), \quad i = I, I-1, \dots, 0. \quad (11)$$

The boundary conditions have to be appropriately included, namely taking (5) instead of (10) for $i = 0$ if $C_0 \geq 0$, and (6) instead of (11) for $i = I$ if $C_I \leq 0$.

We can now summarize the advantages of the first order accurate implicit upwind scheme. The numerical solution is defined by (10) - (11) explicitly as a convex combinations of the neighbor values for arbitrary large Courant numbers. Therefore, the scheme is unconditionally stable and it insures a discrete minimum and maximum principle for any choice of h and τ . This is especially critical if (9) has to be used as the corresponding Courant numbers C_{i^*} or C_{1+i^*} can be arbitrary large.

The main disadvantage is the low accuracy of the method that can be demonstrated for many test examples of practical interest. Therefore, we derive an extension of this method in a form of the second order accurate semi-implicit methods for which the numerical solution can be again determined explicitly.

2.2 Parametric family of second order accurate semi-implicit schemes

We begin by presenting an error term of the first order accurate scheme (4). To do so, we express the values $\phi(x_i, t^n)$ and $\phi(x_{i\pm 1}, t^{n+1})$ using Taylor series at (x_i, t^{n+1}) . First, we have for $t = t^{n+1}$

$$\phi(x_{i\pm 1}, \cdot) = \phi(x_i, \cdot) \pm h \partial_x \phi(x_i, \cdot) + \frac{h^2}{2} \partial_{xx} \phi(x_i, \cdot) + \mathcal{O}(h^3). \quad (12)$$

Second, we have for $x = x_i$

$$\begin{aligned} \phi(\cdot, t^n) &= \phi(\cdot, t^{n+1}) - \tau \partial_t \phi(\cdot, t^{n+1}) + \frac{\tau^2}{2} \partial_{tt} \phi(\cdot, t^{n+1}) + \mathcal{O}(\tau^3) = \\ &\phi(\cdot, t^{n+1}) + \tau v_i \partial_x \phi(\cdot, t^{n+1}) - \frac{\tau^2}{2} v_i \partial_{tx} \phi(\cdot, t^{n+1}) + \mathcal{O}(\tau^3), \end{aligned} \quad (13)$$

where one exploits that $\partial_t \phi = -v \partial_x \phi$ and $\partial_{tt} \phi = -v \partial_{tx} \phi$. Such approach is often called Lax-Wendroff procedure [11]. Opposite to its standard form when all time derivatives in (13) are replaced by spatial derivatives using the equation (1), we allow also the mixed derivatives in (13).

Using (13) and (12) we obtain that the discrete values $\phi(x_i, t^{n+1})$ of exact solution fulfill the first order accurate scheme (4) with the leading error term

$$e_2(x_i, t^{n+1}) := -\frac{\tau^2}{2} v_i \partial_{tx} \phi(x_i, t^{n+1}) + \frac{h\tau}{2} |v_i| \partial_{xx} \phi(x_i, t^{n+1}). \quad (14)$$

Now, to extend the scheme (4) to be second order accurate, we have to approximate the derivatives in e_2 with at least first order accurate approximations. Our aim is to derive a parametric family of semi-implicit upwind schemes that has a convenient stencil in its implicit part and that are unconditionally stable [4].

To do so we define the parametric ‘‘upwind based’’ approximations of $\partial_x \phi(x_i, t^*)$ for $* = n$ or $* = n + 1$,

$$\begin{aligned} h \partial_x^{\alpha-} \phi_i^* &:= \alpha (\phi_i^* - \phi_{i-1}^*) + (1 - \alpha) (\phi_{i+1}^* - \phi_i^*) \\ h \partial_x^{\alpha+} \phi_i^* &:= \alpha (\phi_{i+1}^* - \phi_i^*) + (1 - \alpha) (\phi_i^* - \phi_{i-1}^*). \end{aligned} \quad (15)$$

The approximation $\partial_x^{\alpha-} \phi_i^*$ will be used in (14) if $v_i > 0$ and $\partial_x^{\alpha+} \phi_i^*$ if $v_i < 0$. Additionally, applying the standard backward finite difference for the time derivative, and the upwind finite difference for the spatial derivatives, we obtain

$$\begin{aligned} e_2(x_i, t^{n+1}) &\approx -\frac{\tau}{2} (v_i^+ \partial_x^{\alpha-} + v_i^- \partial_x^{\alpha+}) (\phi_i^{n+1} - \phi_i^n) \\ &+ \frac{\tau}{2} v_i^+ \partial_x^{\alpha-} (\phi_i^{n+1} - \phi_{i-1}^{n+1}) - \frac{\tau}{2} v_i^- \partial_x^{\alpha+} (\phi_{i+1}^{n+1} - \phi_i^{n+1}). \end{aligned}$$

Doing it this way we see that the terms with $\partial_x^{\alpha\mp} \phi_i^{n+1}$ cancel.

Combining now the first order and the second order accurate approximations, we obtain the semi-implicit scheme of the form

$$\begin{aligned} &\phi_i^{n+1} + C_i^+ \left(\phi_i^{n+1} - \phi_{i-1}^{n+1} - \frac{h}{2} \partial_x^{\alpha-} \phi_{i-1}^{n+1} \right) + \\ &C_i^- \left(\phi_{i+1}^{n+1} - \phi_i^{n+1} - \frac{h}{2} \partial_x^{\alpha+} \phi_{i+1}^{n+1} \right) = \phi_i^n - C_i^+ \frac{h}{2} \partial_x^{\alpha-} \phi_i^n - C_i^- \frac{h}{2} \partial_x^{\alpha+} \phi_i^n, \end{aligned} \quad (16)$$

where one can clearly distinguish between the contributions of two approximations having the different order of accuracy. One can write (16) in the concise form using $\mp = -\text{sgn}(C_i)$,

$$\phi_i^{n+1} + |C_i| \left(\phi_i^{n+1} - \phi_{i\mp 1}^{n+1} \mp \frac{h}{2} \partial_x^{\alpha\mp} \phi_{i\mp 1}^{n+1} \right) = \phi_i^n \mp |C_i| \frac{h}{2} \partial_x^{\alpha\mp} \phi_i^n. \quad (17)$$

In [4], using a different parametric form, it is shown that the scheme is unconditionally stable for $\alpha \geq 0$ according to the von Neumann stability analysis. The value $\alpha = 0$ choose “downwind” one-sided finite difference in (15) and $\alpha = 1$ the upwind one. The case $\alpha = 0.5$ results in the central finite difference in (15). In general, the parameters α in (15) can be different for each i and n that we do not emphasize in its notation, but that we exploit later in numerical experiments. In particular, the variable choice

$$\alpha = \frac{2 + |C_i|}{6}, \quad (18)$$

can improve numerical results for many examples as shown in [4] and as confirmed also for other numerical experiments here. The motivation behind (18) is that in the case of constant velocity v in (1) the third order accuracy of (16) can be proved [4].

To obtain the numerical solution ϕ_i^{n+1} from (17), we can write it in the form

$$\begin{aligned} \phi_i^{n+1} = & \left(1 + \frac{1+\alpha}{2} |C_i| \right)^{-1} \left(\phi_{i-1}^{n+1} \frac{1+2\alpha}{2} C_i^+ - \phi_{i-2}^{n+1} \frac{\alpha}{2} C_i^+ \right. \\ & \left. - \phi_{i+1}^{n+1} \frac{1+2\alpha}{2} C_i^- + \phi_{i+2}^{n+1} \frac{\alpha}{2} C_i^- + \phi_i^n - C_i^+ \frac{h}{2} \partial_x^{\alpha-} \phi_i^n - C_i^- \frac{h}{2} \partial_x^{\alpha+} \phi_i^n \right). \end{aligned} \quad (19)$$

Analogously to (4), we can obtain the values ϕ_i^{n+1} from (19) using one forward and one backward substitution, or, similarly to (10) - (11), splitting it into two fractional steps with the prescribed order of the evaluation,

$$\phi_i^{n+1/2} = \frac{2\phi_i^n + \phi_{i-1}^{n+1}(1+2\alpha)C_i^+ - \phi_{i-2}^{n+1}\alpha C_i^+ - C_i^+ h \partial_x^{\alpha-} \phi_i^n}{2 + (1+\alpha)C_i^+}, \quad (20)$$

$$i = 0, 1, \dots, I,$$

$$\phi_i^{n+1} = \frac{2\phi_i^{n+1/2} - \phi_{i+1}^{n+1}(1+2\alpha)C_i^- + \phi_{i+2}^{n+1}\alpha C_i^- - C_i^- h \partial_x^{\alpha+} \phi_i^{n+1/2}}{2 - (1+\alpha)C_i^-}, \quad (21)$$

$$i = I, I-1, \dots, 0.$$

The scheme (20) - (21) represents the explicit form of numerical solution for the proposed family of semi-implicit non-conservative scheme to solve (1). The boundary conditions have to be appropriately included, namely taking (5) instead of (20) for $i = 0$ if $C_0 \geq 0$, and (6) instead of (21) for $i = I$ if $C_I \leq 0$. If for $i = 1$ or $i = I$ one has $C_1 > 0$ or $C_{I-1} < 0$ then one can set $\alpha = 0$ in (20) or (21). In the case that for some i one has $C_i \leq 0$ and $C_{i+1} > 0$, one may use (9) instead.

3 Conservative advection equation

The linear advection equation in the conservative form is written as

$$\partial_t \phi + \partial_x (v\phi) = 0, \quad \phi(x, 0) = \phi^0(x). \quad (22)$$

The same assumptions on the input functions, the initial and boundary conditions as in the non-conservative case apply also here.

To use a conservative finite difference (or a finite volume) method, we divide the interval $(0, L)$ to subintervals (the "control volumes") $(x_{i-1/2}, x_{i+1/2})$, where the "face points" are given by $x_{i+1/2} = ih$, $i = 0, 1, \dots, I$ using the discretization step $h = L/I$. The points x_i are now shifted compared to the notation in Section 2, namely

$$x_i = ih - h/2, \quad i = 1, 2, \dots, I.$$

Our aim is now to find the approximations

$$\Phi_i^n \approx \frac{1}{h} \int_{x_{i-1/2}}^{x_{i+1/2}} \phi(x, t^n) dx \approx \phi(x_i, t^n),$$

for $i = 1, 2, \dots, I$. For the initial conditions, we consider $\Phi_i^0 = \phi^0(x_i)$ that is a second order accurate approximation of the above integrals. The velocity is evaluated in points $x_{i-1/2}$, i.e. $v_{i+1/2} := v(x_{i+1/2})$, in particular the boundary fluxes are given by

$$v_{1/2} = v(x_{1/2}) = v(0), \quad v_{I+1/2} = v(x_{I+1/2}) = v(L).$$

3.1 First order accurate fully implicit scheme

We define the scheme in a locally conservative form

$$\begin{aligned} & \frac{\Phi_i^{n+1} - \Phi_i^n}{\tau} + \\ & \frac{v_{i+1/2}^+ \Phi_i^{n+1} + v_{i+1/2}^- \Phi_{i+1}^{n+1} - v_{i-1/2}^+ \Phi_{i-1}^{n+1} - v_{i-1/2}^- \Phi_i^{n+1}}{h} = 0. \end{aligned} \quad (23)$$

Indexing now the signed Courant numbers at the faces

$$C_{i+1/2} := \frac{\tau v_{i+1/2}}{h}, \quad i = 0, 1, \dots, I,$$

we can rewrite the equations (23) for $i = 1, 2, \dots, I$ to the form

$$\Phi_i^{n+1} = \frac{\Phi_i^n - C_{i+1/2}^- \Phi_{i+1}^{n+1} + C_{i-1/2}^+ \Phi_{i-1}^{n+1}}{1 + C_{i+1/2}^+ - C_{i-1/2}^-}, \quad (24)$$

where we define, formally,

$$\Phi_0^{n+1} = \phi_0(t^{n+1}), \quad \Phi_{I+1}^{n+1} = \phi_L(t^{n+1}).$$

The scheme (24) defines the first order accurate conservative implicit upwind method for (22). The scheme represents a system of linear algebraic equations that can be solved using one forward and one backward substitution as described in the previous section. This can be viewed as the most important advantage of the first order accurate upwind scheme together with its locally conservative form. It is important to note that the case of zero velocity with diverging characteristics as described in Remark 1 is captured by the conservative scheme (24) automatically and no special treatment is required here.

The scheme can be written using two fractional time steps with the prescribed order,

$$\Phi_i^{n+1/2} = \left(1 + C_{i+1/2}^+\right)^{-1} \left(\Phi_i^n + C_{i-1/2}^+ \Phi_{i-1}^{n+1}\right), \quad i = 0, 1, \dots, I$$

$$\Phi_i^{n+1} = \left(1 - C_{i-1/2}^-\right)^{-1} \left(\Phi_i^{n+1/2} - C_{i+1/2}^- \Phi_{i+1}^{n+1}\right), \quad i = I, I-1, \dots, 0.$$

The main disadvantage is again the low accuracy that motivates us to extend the scheme in a form of second order accurate semi-implicit method.

3.2 Parametric class of second order accurate semi-implicit schemes

To derive the error term of the first order accurate scheme (23), we express again the values $\phi(x_i, t^n)$ using Taylor series at (x_i, t^{n+1}) . Instead of (13), we obtain now

$$\begin{aligned} \phi(x_i, t^n) &= \phi(x_i, t^{n+1}) + \\ &\tau \partial_x(v(x_i)\phi(x_i, t^{n+1})) - \frac{\tau^2}{2} \partial_{tx}^2(v(x_i)\phi(x_i, t^{n+1})) + \mathcal{O}(\tau^3), \end{aligned}$$

where we exploited that $\partial_t \phi = -\partial_x(v\phi)$ and $\partial_{tt} \phi = -\partial_{tx}(v\phi)$. Using additionally (12) and

$$v_{i\pm 1/2} = v_i \pm \frac{h}{2} v'_i, \quad \partial_x(v_i \phi(x_i, t^{n+1})) = v_i \partial_x \phi(x_i, t^{n+1}) + v'_i \phi(x_i, t^{n+1}),$$

we obtain the following form of the second order error term

$$e_2(x_i, t^{n+1}) := -\frac{\tau^2}{2} \partial_{tx}^2(v_i \phi(x_i, t^{n+1})) \pm \frac{\tau h}{2} \partial_x(v_i \partial_x \phi(x_i, t^{n+1})),$$

where $\pm = \text{sgn}(v_i)$. Now denoting analogously to (15)

$$\Phi_{i,\alpha-}^* = \alpha \Phi_i^* + (1 - \alpha) \Phi_{i+1}^*, \quad \Phi_{i,\alpha+}^* = (1 - \alpha) \Phi_i^* + \alpha \Phi_{i+1}^*,$$

we can apply the following approximations,

$$\begin{aligned} &\partial_x(v(x_i)\phi(x_i, t^{n+1})) \approx \\ &v_{i+1/2}^+ \Phi_{i,\alpha-}^{n+1} - v_{i-1/2}^+ \Phi_{i-1,\alpha-}^{n+1} + v_{i+1/2}^- \Phi_{i,\alpha+}^{n+1} - v_{i-1/2}^- \Phi_{i-1,\alpha+}^{n+1}, \end{aligned}$$

and

$$hv_{i+1/2}\bar{\partial}_x\phi(x_{i+1/2}, t^{n+1}) \approx v_{i+1/2}^+(\Phi_{i,\alpha-}^{n+1} - \Phi_{i-1,\alpha-}^{n+1}) + v_{i+1/2}^-(\Phi_{i+1,\alpha+}^{n+1} - \Phi_{i,\alpha+}^{n+1}).$$

Together with the above approximations we use the backward finite difference in time and the central difference for the first space derivative in the second term of e_2 . After some algebraic manipulations when several terms cancel, we obtain

$$e(x_i, t^{n+1}) \approx -\frac{\tau}{2h} \left(v_{i+1/2}^+ (\Phi_{i-1,\alpha-}^{n+1} - \Phi_{i,\alpha-}^n) + v_{i+1/2}^- (\Phi_{i+1,\alpha+}^{n+1} - \Phi_{i,\alpha+}^n) - v_{i-1/2}^+ (\Phi_{i-2,\alpha-}^{n+1} - \Phi_{i-1,\alpha-}^n) - v_{i-1/2}^- (\Phi_{i,\alpha+}^{n+1} - \Phi_{i-1,\alpha+}^n) \right).$$

Putting together the first order and the second order approximations, the second order accurate semi-implicit conservative scheme can be written in the form

$$\Phi_i^{n+1} + \frac{\tau}{h} (F_{i+1/2}^{n+1/2} - F_{i-1/2}^{n+1/2}) = \Phi_i^n, \quad (25)$$

where the numerical fluxes for $i = 0, 1, \dots, I$ are defined by

$$F_{i+1/2}^{n+1/2} := v_{i+1/2}^+ \left(\Phi_i^{n+1} - \frac{1}{2}\Phi_{i-1,\alpha-}^{n+1} + \frac{1}{2}\Phi_{i,\alpha-}^n \right) + v_{i+1/2}^- \left(\Phi_{i+1}^{n+1} - \frac{1}{2}\Phi_{i+1,\alpha+}^{n+1} + \frac{1}{2}\Phi_{i,\alpha+}^n \right). \quad (26)$$

Concerning the values Φ_0^{n+1} and Φ_{I+1}^{n+1} that occur in (26) for $i = 1$ if $v_{3/2} > 0$, and for $i = I$ if $v_{I-1/2} < 0$, we use the linear extrapolation,

$$\Phi_0^{n+1} = 2\phi_0(t^{n+1}) - \Phi_1^{n+1}, \quad \Phi_{I+1}^{n+1} = 2\phi_L(t^{n+1}) - \Phi_I^{n+1}. \quad (27)$$

Analogously, if $v_{1/2} < 0$ and $v_{I+1/2} > 0$, we again linearly extrapolate the missing values by

$$\Phi_0^n = 2\phi_0(t^n) - \Phi_1^n, \quad \Phi_{I+1}^n = 2\phi_L(t^n) - \Phi_I^n.$$

Concerning the inflow fluxes $F_{1/2}^{n+1/2}$ and $F_{I+1/2}^{n+1/2}$ at the boundary, we apply a second order accurate approximation, e.g.,

$$F_{1/2}^{n+1/2} = v_{1/2}\phi_0(t^{n+1/2}), \quad \text{if } v_{1/2} \geq 0, \\ F_{I+1/2}^{n+1/2} = v_{I+1/2}\phi_L(t^{n+1/2}), \quad \text{if } v_{I+1/2} \leq 0.$$

We formulate now the scheme (25) in the form suitable for the fast sweeping method. First we substitute (26) to (25),

$$\begin{aligned} & \Phi_i^{n+1} + \frac{1}{2}C_{i+1/2}^+ \left((1+\alpha)\Phi_i^{n+1} - \alpha\Phi_{i-1}^{n+1} + \alpha\Phi_i^n + (1-\alpha)\Phi_{i+1}^n \right) \\ & + \frac{1}{2}C_{i+1/2}^- \left((1+\alpha)\Phi_{i+1}^{n+1} - \alpha\Phi_{i+2}^{n+1} + (1-\alpha)\Phi_i^n + \alpha\Phi_{i+1}^n \right) - \\ & \frac{1}{2}C_{i-1/2}^+ \left((1+\alpha)\Phi_{i-1}^{n+1} - \alpha\Phi_{i-2}^{n+1} + \alpha\Phi_{i-1}^n + (1-\alpha)\Phi_i^n \right) - \\ & \frac{1}{2}C_{i-1/2}^- \left((1+\alpha)\Phi_i^{n+1} - \alpha\Phi_{i+1}^{n+1} + (1-\alpha)\Phi_{i-1}^n + \alpha\Phi_i^n \right) = \Phi_i^n. \end{aligned}$$

Collecting all terms, we can write

$$\begin{aligned} & \left(2 + (1+\alpha)C_{i+1/2}^+ - (1+\alpha)C_{i-1/2}^- \right) \Phi_i^{n+1} = 2\Phi_i^n \quad (28) \\ & + C_{i+1/2}^+ \left(\alpha\Phi_{i-1}^{n+1} - \alpha\Phi_i^n - (1-\alpha)\Phi_{i+1}^n \right) \\ & - C_{i+1/2}^- \left((1+\alpha)\Phi_{i+1}^{n+1} - \alpha\Phi_{i+2}^{n+1} + \alpha\Phi_{i+1}^n + (1-\alpha)\Phi_i^n \right) \\ & + C_{i-1/2}^+ \left((1+\alpha)\Phi_{i-1}^{n+1} - \alpha\Phi_{i-2}^{n+1} + \alpha\Phi_{i-1}^n + (1-\alpha)\Phi_i^n \right) \\ & - C_{i-1/2}^- \left(\alpha\Phi_{i+1}^{n+1} - \alpha\Phi_i^n - (1-\alpha)\Phi_{i-1}^n \right). \end{aligned}$$

Dividing (28) by the term before Φ_i^{n+1} we obtain the formula to be used with the fast sweeping method. In the case that $C_{i-1/2} < 0$ and $C_{i+1/2} > 0$ one can use the first order scheme (24) instead of (28).

For $i = 1$ and $i = I$ we modify the scheme according to the boundary conditions as mentioned before, namely for $i = 1$

$$\begin{aligned} & \left(2 + (1+2\alpha)C_{3/2}^+ - (1+\alpha)C_{1/2}^- \right) \Phi_1^{n+1} = 2\Phi_1^n \quad (29) \\ & + C_{3/2}^+ \left(2\alpha\phi_0(t^{n+1}) - \alpha\Phi_1^n - (1-\alpha)\Phi_2^n \right) \\ & - C_{3/2}^- \left((1+\alpha)\Phi_2^{n+1} - \alpha\Phi_3^{n+1} + \alpha\Phi_2^n + (1-\alpha)\Phi_1^n \right) \\ & + C_{1/2}^+ \phi_0(t^{n+1/2}) - C_{1/2}^- \left(\alpha\Phi_2^{n+1} + (1-2\alpha)\Phi_1^n - 2(1-\alpha)\phi_0(t^n) \right), \end{aligned}$$

and analogously for $i = I$,

$$\begin{aligned} & \left(2 + (1+\alpha)C_{I+1/2}^+ - (1+2\alpha)C_{I-1/2}^- \right) \Phi_I^{n+1} = 2\Phi_I^n \quad (30) \\ & + C_{I+1/2}^+ \left(\alpha\Phi_{I-1}^{n+1} + (1-2\alpha)\Phi_I^n - 2(1-\alpha)\phi_L(t^n) \right) - C_{I+1/2}^- \phi_L(t^{n+1/2}) \\ & + C_{I-1/2}^+ \left((1+\alpha)\Phi_{I-1}^{n+1} - \alpha\Phi_{I-2}^{n+1} + \alpha\Phi_{I-1}^n + (1-\alpha)\Phi_I^n \right) \\ & - C_{I-1/2}^- \left(2\alpha\phi_L(t^{n+1}) - \alpha\Phi_I^n - (1-\alpha)\Phi_{I-1}^n \right). \end{aligned}$$

Note that for $i = 2$ with $C_{3/2} > 0$ and $i = I - 1$ with $C_{I-1/2} < 0$ one has to use also (27).

The derived scheme is exactly mass conservative at the discrete level and it is second order accurate as it is suggested also by numerical experiments. In the case of constant velocity v in (22) the scheme is equivalent to the parametric family of nonconservative semi-implicit scheme (19) when also the von Neumann unconditional stability is valid.

We note that although the parameter α can be chosen freely in each time interval, e.g. $\alpha \in [0, 1]$, it shall not vary with respect to i if the discrete form of local mass balance property shall be fulfilled.

4 Two dimensional case

We now apply the so called Strang splitting to solve the non-conservative advection equation in two-dimensional case, but the idea can be applied in more dimensional cases and for the conservative form, too.

The advection equation is now given in the form

$$\partial_t \phi + \vec{v} \cdot \nabla \phi = 0, \quad \phi(x, y, 0) = \phi^0(x, y), (x, y) \in \Omega, \quad (31)$$

where $\Omega \subset R^2$ takes here a simple form of a square and $\vec{v} = (v_1(x, y), v_2(x, y))$ is a given velocity vector field. The boundary conditions are defined depending on the flow regime at the boundary $\partial\Omega$ with the values prescribed only at the inflow part,

$$\phi(x, y, t) = \phi_{in}(x, y, t) \text{ if } \vec{n}(x, y) \cdot \vec{v}(x, y) \leq 0, (x, y) \in \partial\Omega, \quad (32)$$

where \vec{n} is the outward normal vector.

We use analogous notation to derive numerical approximations as in the previous section with the addition that $y_j = jh$ for $j = 0, 1, \dots, I$. Furthermore, we denote $t^{n+1/2} = t^n + \tau/2$.

The idea of the time splitting method is to approximate and split the problem (31) into two subproblems that are coupled only by the choice of initial conditions, and that are solved separately in a specified sequence. Let us explain the simplest variant in details.

The first subproblem takes the form of one dimensional advection equations for the parameter $y \in (0, L)$,

$$\partial_t \phi(x, y, t) + v_1(x, y) \partial_x \phi(x, y, t) = 0, \quad x \in (0, L), \quad (33)$$

and the second subproblem takes the analogous form for the parameter $x \in (0, L)$,

$$\partial_t \phi(x, y, t) + v_2(x, y) \partial_y \phi(x, y, t) = 0, \quad y \in (0, L). \quad (34)$$

The splitting in time is realized as follows. Let the solution $\phi(x, y, t^n)$ (or its approximation) of (31) be available at some time $t = t^n$, $0 \leq n < N$. To obtain an approximation of $\phi(x, y, t^{n+1})$ we do three steps. First, the subproblem (33)

is solved for $t \in (t^n, t^{n+1/2})$ with the initial condition defined by $\phi(x, y, t^n)$. Afterwards, the subproblem (34) is solved for $t \in (t^n, t^{n+1})$ with the initial condition defined by the solution of (33) at $t = t^{n+1/2}$. Finally, the subproblem (33) is solved now for $t \in (t^{n+1/2}, t^{n+1})$ with the initial condition defined by the solution of (34) at $t = t^{n+1}$. The result is the desired approximation of $\phi(x, y, t^{n+1})$.

To discretize the advection equation (31) also in space, we consider the first subproblem (33) only for $y = y_j$, $j = 0, 1, \dots, J$, and the second one (34) only for $x = x_i$, $i = 0, 1, \dots, I$. For the resulting one-dimensional advection problems we can apply the numerical method from the previous section, when each of the resulting discrete algebraic systems can be solved in one forward and one backward substitution.

5 Numerical experiments

In following numerical experiments we want to illustrate the properties of the derived semi-implicit schemes using some standard benchmarks. For the non-conservative advection, the methods are implemented in C-language for two-dimensional problems. The numerical solutions of one-dimensional conservative advection is implemented in Python. The experiments with optimized choice of parameters using automatic differentiation is realized with Python and its library PyTorch.

For examples having available exact solution on a whole time interval we compute the global discrete L_1 errors E that takes in one-dimensional case the form

$$E = E(h, \tau) = h\tau \sum_{i,n} |\phi_i^n - \phi(x_i, t^n)| \quad (35)$$

and analogously for two-dimensional case. If an exact solution is available only at the final time $t^N = T$, we compute the error in the form

$$E^N = E^N(h, \tau) = h \sum_i |\phi_i^N - \phi(x_i, T)| \quad (36)$$

and analogously in two-dimensional case.

5.1 One dimensional nonconservative advection

The following example contains all important features of the non-conservative linear advection equation (1) with variable velocity and general boundary conditions (2). The velocity changes its sign twice inside of computational interval with converging and expanding characteristics and it prescribes variable inflow and outflow boundary conditions.

The example is formally treated as two-dimensional. The computational domain is $\Omega = (-\pi/2, 3\pi/2)^2$, the initial function $\phi(x, y, 0) = \sin(x)$ and $T = 1.2$. The velocity function $\vec{v} = (v_1(x, y), v_2(x, y))$ is depending on the

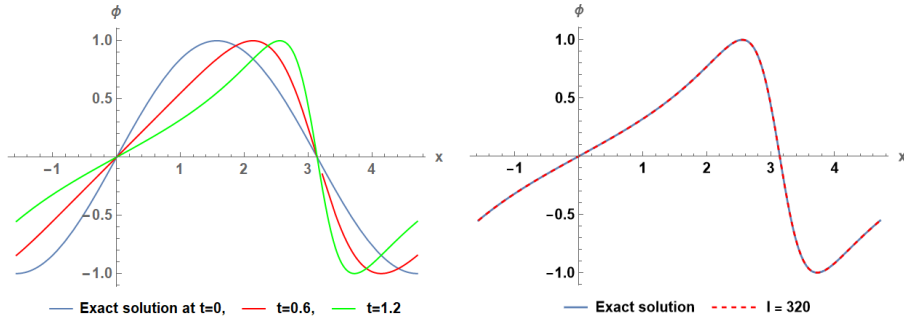


Fig. 1 The exact solution for $t = 0$, $t = T/2$, and $t = T$ (left) and the comparison of exact and numerical solution at $t = T$ (right) for the example 5.1.

spatial coordinate x only with $v_1(x, y) = \sin(x)$ and $v_2(x, y) = 0$. The exact solution is given by

$$\phi = \sin(2 \arctan(e^{-t} \tan(x/2))).$$

We solve the example with discretization steps resulting in the maximal Courant number being approximately 3.81. In Table 1 we present the global discrete errors E in (35) for two interesting choices of the parameter α , namely $\alpha = 0.5$ and α defined by (18). One can see that the results are of a good accuracy even for Courant number larger than 1. The EOC is approaching 2 from above in both cases with the results for the variable α slightly better than for the fixed value.

I	N	$E, \alpha = 0.5$	EOC	E, α in (18)	EOC
40	1	0.810861	-	0.556925	-
80	2	0.167179	2.278	0.099711	2.481
160	4	0.035211	2.247	0.018519	2.428
320	8	0.007858	2.163	0.003831	2.273

Table 1 Numerical errors and EOC for two choice of α in example 5.1.

Finally, we compute the example on the finest mesh using only one time step resulting in the maximal Courant number being approximately 30.5. The obtained numerical solution is compared with the one obtained on the coarsest mesh in Figure 2. One can see that the large Courant numbers do not result in any instabilities.

5.2 Optimization of parameters by automatic differentiation

To illustrate the possibilities of variable parameter $\alpha = \alpha_i^n$ in (17), we compute an example with variable velocity, where we let the code optimize the

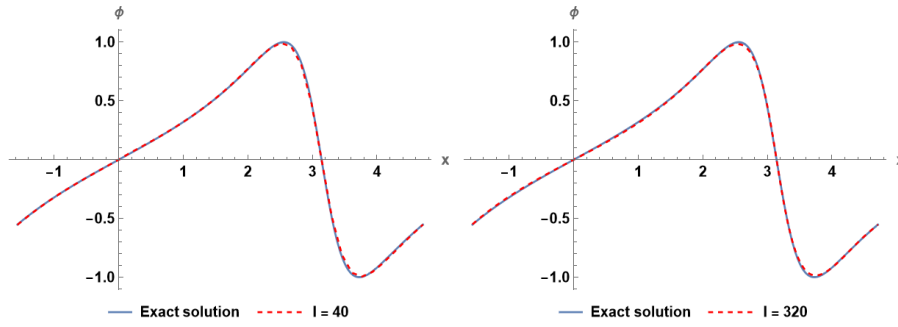


Fig. 2 Comparison of exact and numerical solutions obtained only with one time step for example 5.1. The maximal Courant number is 3.81 (left) and 30.5 (right).

values of α_i^n at each time step and at each grid point. To do so we use the library PyTorch [16] to implement a straightforward gradient descent method to minimize the loss function

$$J = J(I, N) = h\tau \sum_{i,n} (\min\{0, \phi_i^n\})^2$$

with respect to parameters α_i^n .

In particular, we set initially $\alpha_i^n = 0.5$ for $i = 1, 2, \dots, I - 1$ and $n = 1, 2, \dots, N - 1$ for which we compute the values ϕ_i^n of numerical solution. Afterwards using the automatic differentiation available in PyTorch we obtain the gradient of J with respect to all values of α_i^n . Next we subtract the gradient multiplied by a parameter (the "learning rate") η from the values of α_i^n that results in a smaller value of J . In theory, one can continue with this procedure up to a point when the decrease of J is not substantial. In our case, we use only one step of such optimization.

To show clearly this idea we choose the following example. The domain is $\Omega = (-2, 12)$, $T = 2\pi/\sqrt{3}$, the initial function $\phi(x, 0) = \exp(-2x^2)$ and the velocity function $v(x) = 2 + \sin(x)$. One can show that $\phi(x, T) = \phi^0(x - 2\pi)$.

In Table 2 we summarize the results. For three consecutively refined meshes we present the value of J before and after the optimization step, and analogously the errors E^N in (36). One can see that the unphysical oscillations can be decreased significantly with a slight improvement in the precision.

I	N	$\eta \cdot 10^6$	$J_b \cdot 10^{-3}$	$J_a \cdot 10^{-3}$	E_b^N	E_a^N
70	50	0.2	3.68	0.0768	0.521	0.511
140	100	8.0	1.12	0.0156	0.197	0.190
280	200	160.0	0.0664	0.00354	0.0533	0.0448

Table 2 The learning rate η , the values of the loss function J , and the errors E^N in (36) using three meshes for example 5.2. The indices b and a means "before" and "after" optimization.

To show the influence of optimized values α visually, we present the figures for $I = 70$ and $N = 50$ representing a rather coarse time and space discretization. In Figure 3 we present the numerical solutions at $t^{N/2} = T/2$ and $t^N = T$ for the fixed choice of all $\alpha_i^n \equiv 0.5$ when one can observe clearly some unphysical negative values. Furthermore, the numerical solutions at the same times obtained after one optimization step are plotted together with the values of $\alpha_i^{N/2}$ and α_i^N . One can clearly observe that the largest unphysical oscillation are suppressed. Analogously, the same results are presented also for the refined discretization steps with $I = 140$ and $N = 100$.

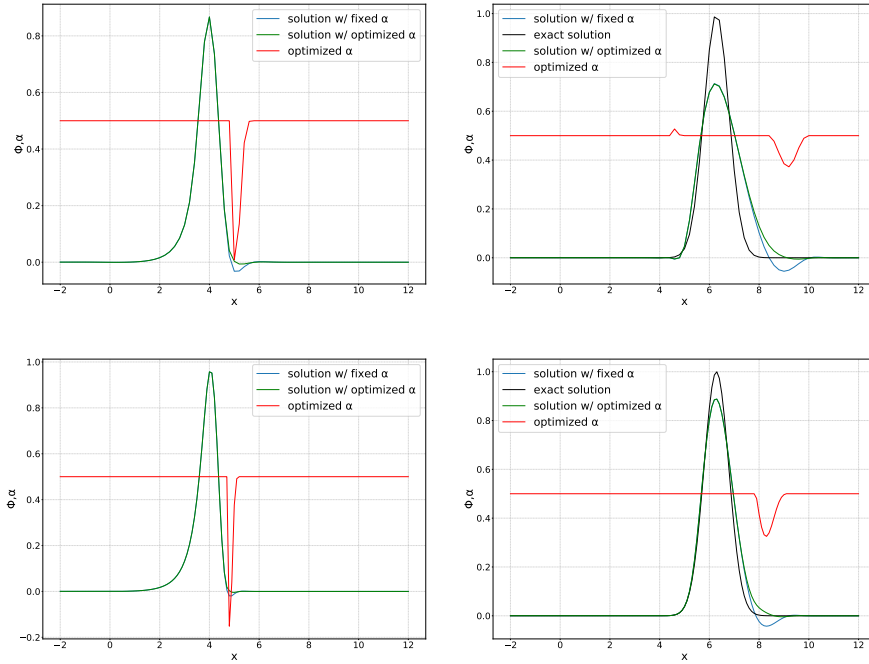


Fig. 3 Numerical solution and variable parameters for $t = T/2$ (left) and for $t = T$ (right) for example 5.2. The top row is obtained with $I = 70$ and the bottom one with $I = 140$.

5.3 One dimensional conservative advection

The following example illustrates the applicability of semi-implicit scheme for the advection equation in the conservative form (22). To check the mass conservation property, we choose an example with zero velocity at boundary points. Inside of the computational interval $\Omega = (-\frac{\pi}{2}, \frac{5\pi}{2})$ the variable velocity $v(x) = \cos(x)$ changes twice its sign. The initial condition has the form

$\phi(x, 0) = \cos(x)$ and $T = 1$. The exact solution is given by

$$\phi = \cos^2 \left(2 \tan^{-1} \left(\tanh \left(\frac{1}{2} \left(t - 2 \tanh^{-1} \left(\tan \left(\frac{x}{2} \right) \right) \right) \right) \right) \right),$$

see the left picture in Figure 4.

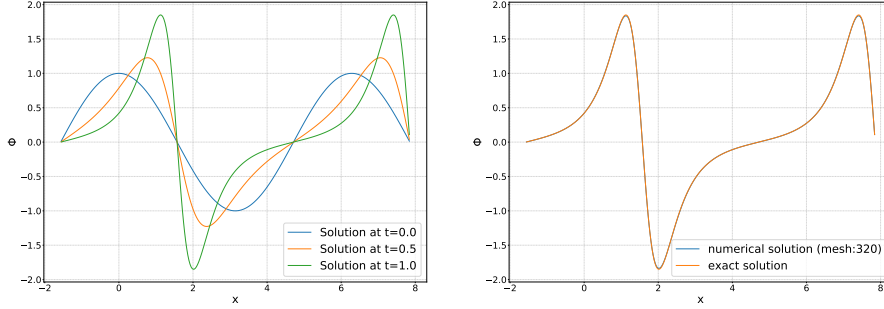


Fig. 4 The exact solution at $t = 0$, $t = T/2$, and $t = T$ (left) and the comparison of exact and numerical solution at $t = T$ (right) for example 5.3.

We solve the example with discretization steps such that the maximal Courant number is approximately 4.24. The global discrete errors E in (35) are presented in Table 5.3 for $\alpha = 0.5$ and $\alpha = 1$. The numerical results are stable even for Courant number larger than 1, see the right picture in Figure 4 for a visual comparison. The EOC is approximately 2 in both cases with the choice $\alpha = 1$, as expected, being slightly better for the example with larger Courant numbers.

I	N	$E, \alpha = 0.5$	EOC	$E, \alpha = 1$	EOC
40	1	0.9610	-	0.7013	-
80	2	0.2750	1.81	0.1941	1.85
160	4	0.0651	2.08	0.0442	2.13
320	8	0.0150	2.12	0.0098	2.17

Table 3 Numerical errors for example 5.3 with the maximal Courant number 4.

In Table 5.3 we present the results for the same example with the four times smaller time step resulting in the maximal Courant number being approximately 1. Of course, the precision of results increases, and, moreover, the choice $\alpha = 0.5$ gives now better results than the choice $\alpha = 1$.

Note that we always obtain a perfect mass conservation at the discrete level by checking

$$\sum_i \Phi_i^n = \sum_i \Phi_i^0, \quad n = 1, 2, \dots, N$$

I	N	$E, \alpha = 0.5$	EOC	$E, \alpha = 1$	EOC
40	4	0.1181	-	0.1683	-
80	8	0.0256	2.20	0.0461	1.87
160	16	0.0054	2.26	0.011	2.02
320	32	0.0012	2.16	0.0028	2.02

Table 4 Numerical errors for example 5.3 with the maximal Courant number 1.

with a difference given only by rounding errors around 10^{-15} .

Finally, to illustrate the stability of our scheme, we compute the example on the finest mesh with only one time step resulting in the maximal Courant number approximately 34, see the right picture in Figure 5 with no instabilities occurring.

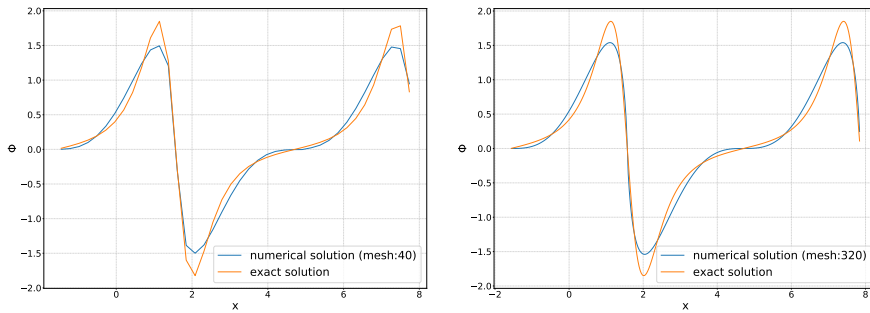


Fig. 5 Numerical solutions obtained with only one time step for example 5.3. The maximal Courant number equals 4.24 (left) and 33.95 (right).

5.4 Two-dimensional example with diagonally variable velocity

With the next example we solve an analogous problem to Example 5.1 with the velocity $\vec{v} = (\sin(2\pi(x+y)/2), \sin(2\pi(x+y)/2))$ that is variable only in a diagonal direction of the domain $\Omega = (-1, 2) \times (-1, 2)$. We use the initial condition $\phi(x, y, 0) = \sin(2\pi(x+y)/2)$ and $T = 0.24$.

The example is chosen to test the accuracy of the operator splitting method as described in Section 4. To compute the global error E analogous to (35) we use always a half time step twice in the subproblem (33) when compared to the time step of subproblem (34) as described in Section 4. Consequently, the maximal Courant number in the x direction is a half of the maximal Courant number in y direction. Note that for explicit methods a typical stability restriction is given by the sum of directional Courant numbers that is required to be smaller than one [11]. We compute the example with the maximal Courant number in y direction being 1.6.

The exact solution is given by

$$\phi = \sin\left(2 \arctan\left(e^{-2\pi t} \tan\left(\pi \frac{x+y}{2}\right)\right)\right).$$

The numerical results are presented in Figure 6 and 7 and in Table 5. We see that the method for two typical choices of parameter α are second order accurate for this example.

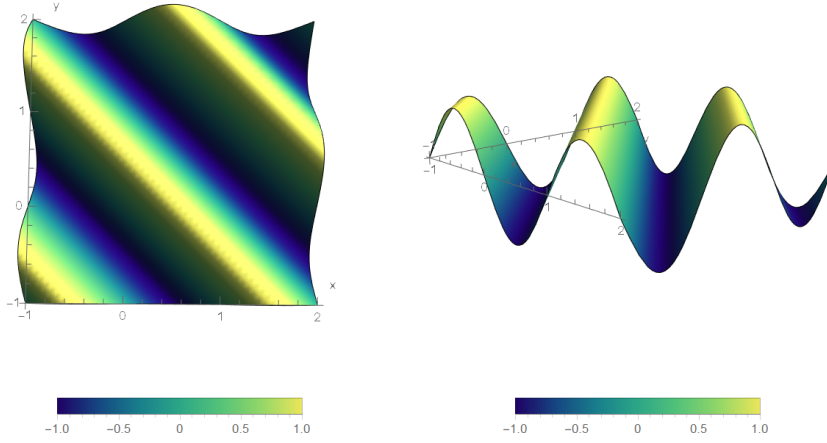


Fig. 6 The initial condition for Example 5.4 viewed from a top and a side.

I	N	$E, \alpha = 0$	EOC	E, α in (18)	EOC
20	1	0.0874	-	0.0838	-
40	2	0.0179	2.29	0.0173	2.27
80	4	0.00319	2.49	0.00302	2.52
160	8	0.000624	2.36	0.000569	2.41

Table 5 Numerical errors for two choices of α for example 5.4.

5.5 Example with deformation velocity

To test our method for a nontrivial case, we choose two-dimensional example with a deformation velocity in which the initial profile of solution is deformed significantly in time. For this example we check quantitatively not only the numerical errors, but also two other numerical artifacts - negative unphysical oscillations and a violation of mass conservation in a discrete form. As we

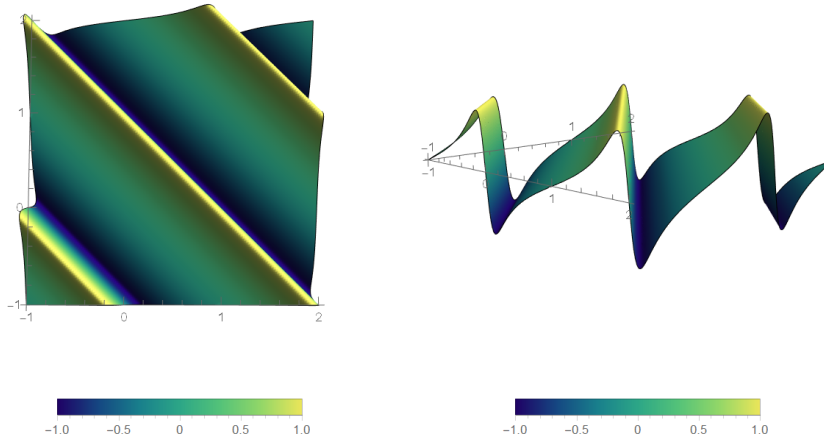


Fig. 7 The numerical solution for Example 5.4 in time $t = T$ for $I = 160$ viewed from a top and a side.

show, the both of them are visible for a coarse mesh, but these numerical errors decrease rapidly with the mesh refinement.

The domain is the unit square $\Omega = (0, 1) \times (0, 1)$ and $T = 1$. The velocity vector \vec{v} , see Figure 8, is defined by

$$\begin{aligned} v_1(x, y, t) &= -4 \cos(\pi t) \sin^2(2\pi x) \sin(2\pi y) \cos(2\pi y), \\ v_2(x, y, t) &= 4 \cos(\pi t) \sin^2(2\pi y) \sin(2\pi x) \cos(2\pi x). \end{aligned}$$

Note that the time dependency of \vec{v} in numerical simulations is resolved by evaluating v for each n at $t = t^n + \tau/2$. The velocity has the zero divergence and it is equal zero at the boundary, so the integral of the initial function (the mass) shall be conserved in time.

We consider two different initial conditions in this example, see Figure 9. First, the Gaussian is chosen

$$\phi(x, y, 0) = e^{-100((x-0.5)^2 + (y-0.5)^2)}, \quad (37)$$

and, second, the signed distance function is considered,

$$\phi(x, y, 0) = \sqrt{(x-0.5)^2 + (y-0.5)^2}. \quad (38)$$

In both cases, the initial profile of the solution ϕ is deformed up to time $t = 0.5$ when the direction of velocity change its sign, so the deformation is reversed afterwards and the initial profile shall be recovered at time $t = 1$.

We compute the example with maximal Courant numbers being 0.76 in y -direction. The numerical solutions for the finest mesh at the time of maximal deformation are plotted in Figure 10 and, moreover, at the final time when the initial profile should be reproduced, see Figure 11. In Tables 6 and 7 we

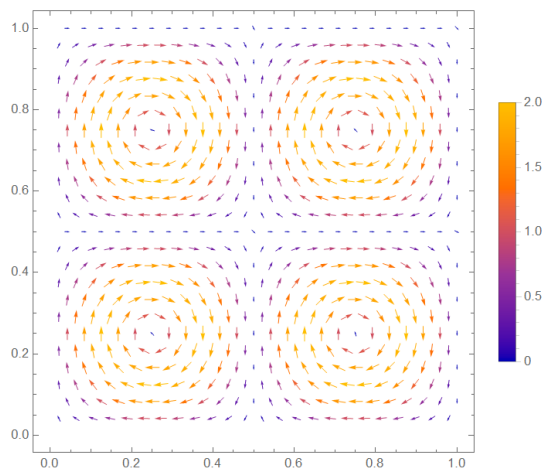


Fig. 8 The velocity field \vec{v} at $t = 0$ for example 5.5.

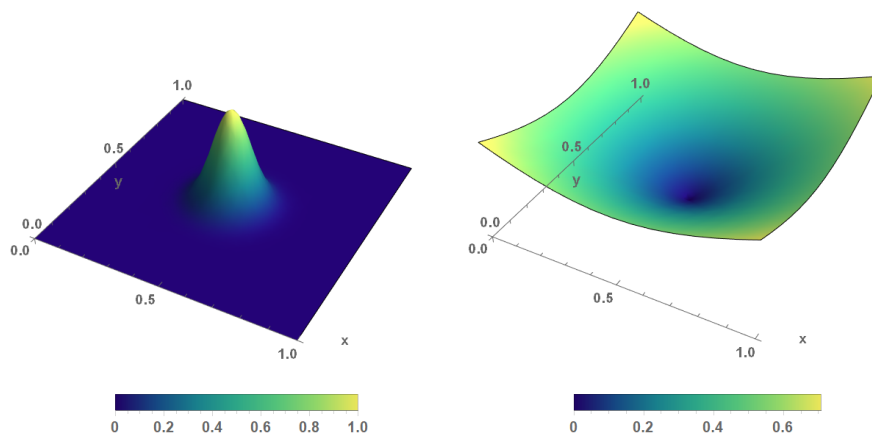


Fig. 9 Initial profiles (37) (left) and (38) (right) for example 5.5.

compute the error E^N analogous to (36) obtained for each numerical solution as the difference between its values at the initial and the final time.

Next we evaluate the numerical artifact in the form of unphysical negative oscillations in the case of initial condition (37). We plot the minimal value for each numerical solution per each time step at all grid levels in Figure 5.5. We note that the extremal (rounded) values for each mesh with respect to n are -0.0677 , -0.0275 , -0.0108 , and -0.00163 from the coarsest to the finest mesh.

Finally, the plot of a difference between the initial (conserved) mass and the actual one at each time step for all grid levels can be found in Figure 5.5.

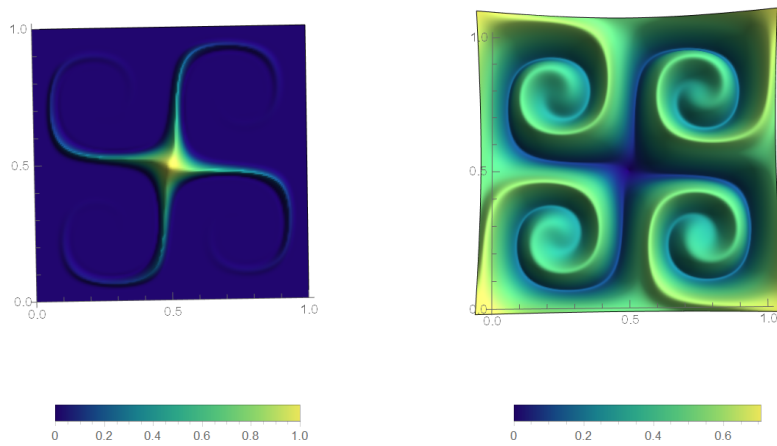


Fig. 10 The maximal deformation at $t = 0.5$ for (37) (left) and (38) (right) for example 5.5.

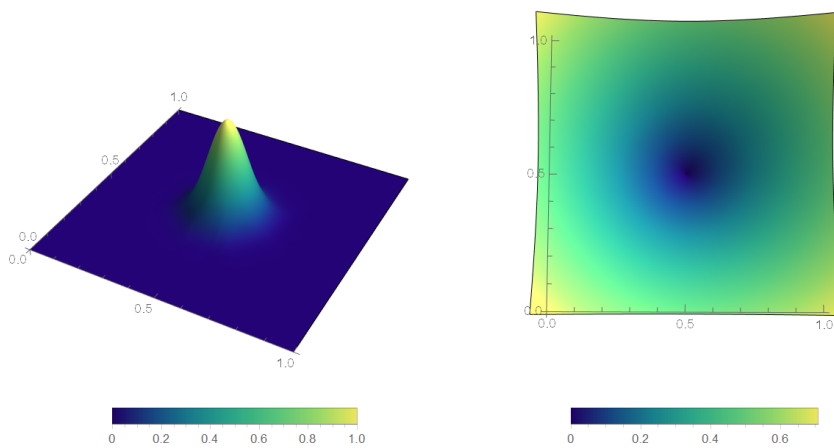


Fig. 11 Solution at $t = 1$ and $I = 320$ for (37) (left) and (38) (right) for example 5.5

Note that the initial mass (the integral of initial function) is approximated by the value 0.031416 for (37) and $n = 0$ using

$$M = M(I, n) = h^2 \sum_{i,j} \phi_{ij}^n. \quad (39)$$

I	Δt	$E, \alpha = 0.5$	EOC	E, α in (18)	EOC
40	100	0.01088	-	0.00928	-
80	200	0.00507	1.10	0.00415	1.16
160	400	0.00177	1.52	0.00138	1.59
320	800	0.00042	2.09	0.00030	2.18

Table 6 Numerical error E^N in (36) for the initial condition (37) in example 5.5.

I	Δt	$E, \alpha = 0.5$	EOC	E, α in (18)	EOC
40	100	0.01692	-	0.01355	-
80	200	0.00458	1.89	0.00351	1.95
160	400	0.00092	2.32	0.00067	2.38
320	800	0.00014	2.76	0.00001	2.80

Table 7 Numerical errors E^N in (36) with the initial condition (38) in example 5.5.

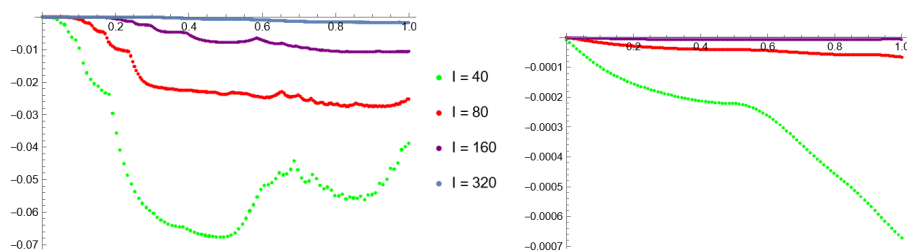


Fig. 12 The minimum (left) and the difference to the initial mass (right) for numerical solution of example 5.5.

6 Conclusions

We present the novel semi-implicit parametric family of one-dimensional numerical schemes for conservative and non-conservative advection equation. Using the Strang splitting for the advection in several dimensions, one can obtain the numerical solutions of advection equations using an (in advance known) fixed number of alternating substitutions. As the schemes are second order accurate in time and space with unconditional von Neumann stability, they can be considered as a good alternative to standard explicit and implicit schemes for advection dominated problems.

References

1. Arbogast, T., Huang, C.S., Zhao, X., King, D.N.: A third order, implicit, finite volume, adaptive Runge–Kutta WENO scheme for advection–diffusion equations. *Computer Methods in Applied Mechanics and Engineering* **368**, 113–155 (2020)
2. Carciopolo, L.D., Bonaventura, L., Scotti, A., Formaggia, L.: A conservative implicit multirate method for hyperbolic problems. *Computational Geosciences* **23**(4), 647–664 (2019)

3. Frolkovič, P., Lampe, M., Wittum, G.: Numerical simulation of contaminant transport in groundwater using software tools of r^3t . *Computing and Visualization in Science* **18**(1), 17–29 (2016)
4. Frolkovič, P., Mikula, K.: Semi-implicit second order schemes for numerical solution of level set advection equation on Cartesian grids. *Applied Mathematics and Computation* **329**, 129–142 (2018)
5. Fuhrmann, J., Langmach, H.: Stability and existence of solutions of time-implicit finite volume schemes for viscous nonlinear conservation laws. *Applied Numerical Mathematics* **37**(1-2), 201–230 (2001)
6. Hadjimichael, Y., Ketcheson, D.I., Lóczy, L.: Positivity preservation of implicit discretizations of the advection equation. arXiv preprint arXiv:2105.07403 (2021)
7. Hahn, J., Mikula, K., Frolkovič, P., Medl'a, M., Basara, B.: Iterative inflow-implicit outflow-explicit finite volume scheme for level-set equations on polyhedron meshes. *Computers & Mathematics with Applications* **77**(6), 1639–1654 (2019)
8. Ibolya, G., Mikula, K.: Numerical solution of the 1d viscous Burgers' and traffic flow equations by the inflow-implicit/outflow-explicit finite volume method. In: *Proceedings of ALGORITMY*, pp. 191–200. STU Bratislava (2020)
9. Izzo, G., Jackiewicz, Z.: Highly stable implicit–explicit Runge–Kutta methods. *Applied Numerical Mathematics* **113**, 71–92 (2017)
10. Knodel, M.M., Kräutle, S., Knabner, P.: Global implicit solver for multiphase multi-component flow in porous media with multiple gas phases and general reactions. In: *International Conference on Finite Volumes for Complex Applications*, pp. 595–603. Springer (2020)
11. LeVeque, R.J.: *Finite volume methods for hyperbolic problems*, vol. 31. Cambridge university press (2002)
12. Lozano, E., Aslam, T.D.: Implicit fast sweeping method for hyperbolic systems of conservation laws. *Journal of Computational Physics* **430**, 110039 (2021)
13. May, S., Berger, M.: An explicit implicit scheme for cut cells in embedded boundary meshes. *Journal of Scientific Computing* **71**(3), 919–943 (2017)
14. Mikula, K., Ohlberger, M., Urbán, J.: Inflow-implicit/outflow-explicit finite volume methods for solving advection equations. *Applied Numerical Mathematics* **85**, 16–37 (2014)
15. Pártl, O., Beneš, M., Frolkovič, P., Illangasekare, T., Smits, K.: Numerical modeling of non-isothermal gas flow and NAPL vapor transport in soil. *Computer Physics Communications* **202**, 175–187 (2016)
16. Paszke, A., et. al.: Pytorch: An imperative style, high-performance deep learning library. In: H. Wallach, et. al. (eds.) *Advances in Neural Information Processing Systems 32*, pp. 8024–8035. Curran Associates, Inc. (2019)
17. Polívka, O., Mikyška, J.: Compositional modeling in porous media using constant volume flash and flux computation without the need for phase identification. *Journal of Computational Physics* **272**, 149–169 (2014)
18. Puppo, G., Semplice, M., Visconti, G.: Quinpi: integrating conservation laws with CWENO implicit methods. arXiv preprint arXiv:2102.00741 (2021)
19. Qin, T., Shu, C.W.: Implicit positivity-preserving high-order discontinuous Galerkin methods for conservation laws. *SIAM Journal on Scientific Computing* **40**(1), A81–A107 (2018)
20. Radu, F.A., Pop, I.S., Attinger, S.: Analysis of an Euler implicit-mixed finite element scheme for reactive solute transport in porous media. *Numerical Methods for Partial Differential Equations: An International Journal* **26**(2), 320–344 (2010)
21. Uçar, Y., Yağmurlu, N.M., Çelikkaya, İ.: Operator splitting for numerical solution of the modified Burgers' equation using finite element method. *Numerical Methods for Partial Differential Equations* **35**(2), 478–492 (2019)
22. Zhang, L., Ge, Y.: Numerical solution of nonlinear advection diffusion reaction equation using high-order compact difference method. *Applied Numerical Mathematics* **166**, 127–145 (2021)
23. Zhao, H.: A fast sweeping method for eikonal equations. *Mathematics of computation* **74**(250), 603–627 (2005)